

AD-A232 828

DTIC FILE COPY

2

OFFICE OF NAVAL RESEARCH

Contract N00014-87-J-1118

R & T Code 4133016

Technical Report No. 18

**A Raman Spectroscopic and Electrochemical Study of the  
Photoinduced Crystallization of Triethylenediamine Triiodide**

**Upon a Silver Electrode**

by

**T. Ozeki and D.E. Irish**

**Prepared for Publication**

in

**Journal of Physical Chemistry**

DTIC  
ELECTE  
MAR 15 1991  
S B D

**Guelph-Waterloo Center for Graduate Work in Chemistry  
Waterloo Campus  
Department of Chemistry  
University of Waterloo  
Waterloo, Ontario  
Canada, N2L 3G1**

**February 15, 1991**

**Reproduction in whole or in part is permitted for  
any purpose of the United States Government**

**\*This document has been approved for public release  
and sale; its distribution is unlimited.**

91 3 11 048

## REPORT DOCUMENTATION PAGE

1a. REPORT SECURITY CLASSIFICATION Unclassified			1b. RESTRICTIVE MARKINGS		
2a. SECURITY CLASSIFICATION AUTHORITY Unclassified			3. DISTRIBUTION / AVAILABILITY OF REPORT Public Release/Unlimited		
2b. DECLASSIFICATION / DOWNGRADING SCHEDULE					
4. PERFORMING ORGANIZATION REPORT NUMBER(S) ONR Technical Report #18			5. MONITORING ORGANIZATION REPORT NUMBER(S)		
6a. NAME OF PERFORMING ORGANIZATION D. E. Irish University of Waterloo		6b. OFFICE SYMBOL (If applicable)		7a. NAME OF MONITORING ORGANIZATION Office of Naval Research	
6c. ADDRESS (City, State, and ZIP Code) Department of Chemistry University of Waterloo Waterloo, Ontario, Canada, N2L 3G1		7b. ADDRESS (City, State, and ZIP Code) The Ohio State University, Research Center 1314 Kinnear Road, Room 318 Columbus, Ohio, U.S.A., 43212-1194			
8a. NAME OF FUNDING / SPONSORING ORGANIZATION Office of Naval Research		8b. OFFICE SYMBOL (If applicable)		9. PROCUREMENT INSTRUMENT IDENTIFICATION NUMBER N00014-87-J-1118	
8c. ADDRESS (City, State, and ZIP Code) Chemistry Division 800 N. Quincy Street Arlington, VA, U.S.A., 22217-5000		10. SOURCE OF FUNDING NUMBERS			
		PROGRAM ELEMENT NO.		PROJECT NO.	TASK NO.
				WORK UNIT ACCESSION NO.	
11. TITLE (Include Security Classification) A Raman Spectroscopic and Electrochemical Study of the Photoinduced Crystallization of Triethylenediamine Triiodide Upon a Silver Electrode					
12. PERSONAL AUTHOR(S) T. Ozeki and D.E. Irish					
13a. TYPE OF REPORT Technical		13b. TIME COVERED FROM 08/90 TO 12/90		14. DATE OF REPORT (Year, Month, Day) 1990-02-15	
15. PAGE COUNT 25					
16. SUPPLEMENTARY NOTATION Submitted to Journal of Physical Chemistry					
17. COSATI CODES			18. SUBJECT TERMS (Continue on reverse if necessary and identify by block number)		
FIELD	GROUP	SUB-GROUP	Photon induced crystallization; Raman spectroscopy; diprotonated DABCO triiodide; electrochemistry		
19. ABSTRACT (Continue on reverse if necessary and identify by block number)					
<p>When a silver electrode, electrochemically coated with AgI, is immersed in an electrolyte containing NaI and the diprotonated form of 1,4-diazabicyclo[2.2.2]octane (abbreviated DABCO-<math>H_2^{2+}</math>), and is bathed in 514.5 nm radiation from an argon ion laser through the objective of the microscope attachment of the DILOR Omars-89 Raman spectrophotometer, crystals form from the focal point. These are attributed to DABCO-<math>H_2^{2+} \cdot 2I_3^-</math>. Both spectroscopic and electrochemical experiments are described and interrelated. A mechanism for this photoinduced electrochemical crystal growth is presented.</p>					
20. DISTRIBUTION / AVAILABILITY OF ABSTRACT <input checked="" type="checkbox"/> UNCLASSIFIED/UNLIMITED <input type="checkbox"/> SAME AS RPT. <input type="checkbox"/> DTIC USERS			21. ABSTRACT SECURITY CLASSIFICATION Unclassified		
22a. NAME OF RESPONSIBLE INDIVIDUAL Dr. Robert J. Nowak			22b. TELEPHONE (Include Area Code) (519) 885-1211, ext. 2500		22c. OFFICE SYMBOL

**A RAMAN SPECTROSCOPIC AND ELECTROCHEMICAL STUDY OF THE  
PHOTOINDUCED CRYSTALLIZATION OF TRIETHYLENEDIAMINE  
TRIIODIDE UPON A SILVER ELECTRODE**

Toru Ozeki<sup>†</sup> and Donald E. Irish<sup>\*</sup>

<sup>\*</sup>Department of Chemistry  
University of Waterloo  
Waterloo, Ontario  
Canada N2L 3G1

<sup>†</sup>Present Address:  
Hyogo University of Teacher Education  
942-1 Shimokume  
Yashiro-cho, Kato-gun  
Hyogo, Japan 673-14

**Abstract**

When a silver electrode, electrochemically coated with AgI, is immersed in an electrolyte containing NaI and the diprotonated form of 1,4-diazabicyclo[2.2.2]octane (abbreviated DABCO-H<sub>2</sub><sup>2+</sup>), and is bathed in 514.5 nm radiation from an argon ion laser through the objective of the microscope attachment of the DILOR Omars-89 Raman spectrophotometer, crystals form from the focal point. These are attributed to DABCO-H<sub>2</sub><sup>2+</sup>·2I<sub>3</sub><sup>-</sup>. Both spectroscopic and electrochemical experiments are described and interrelated. A mechanism for this photoinduced electrochemical crystal growth is presented.



Accession For	
NTIS GRA&I	<input checked="checked" type="checkbox"/>
DTIC TAB	<input type="checkbox"/>
Unannounced	<input type="checkbox"/>
Justification	
By	
Distribution/	
Availability Codes	
Dist	Avail and/or Special
A-1	

## **Introduction**

Surface enhanced Raman scattering (SERS) from triethylenediamine (or 1,4-diazabicyclo[2.2.2]octane, called DABCO for short) adsorbed on a silver electrode from an aqueous solution has been extensively studied in our laboratory.<sup>1-4</sup> These experiments included the measurement of potential and excitation profiles<sup>1,2</sup> and the dependence on pH (and thus the degree of protonation) and on background electrolyte.<sup>3</sup> The spectra of the unprotonated, cage-like, molecule support the view that a photon-driven charge-transfer mechanism plays a role in SERS in addition to the electromagnetic enhancement mechanism, which is always operative.<sup>1,2</sup> The vibrational spectra of these molecules were also measured.<sup>4</sup> Subsequent experiments have been carried out in an electrochemical cell designed for use under the objective lens of the Raman microscope. Under these conditions the Raman spectrum of an acidic solution containing DABCO and sodium iodide contained lines which were not characteristic of DABCO or electrode-adsorbed iodide. These new lines are attributed to the diprotonated DABCO triiodide crystal, formed, attached, and growing from a laser-irradiated site on the silver electrode. This so-called 'photoinduced electrochemical crystal growth' is described in this article.

## **Experimental**

A Dilor OMARS-89 spectrometer with a 512 channel diode array optical multichannel analyzer and microscope accessory, interfaced to an IBM-PC-AT computer, was used for the measurements. As excitation light sources, the 514.5 nm line of the Coherent Innova 70 argon ion laser and the 633.1 nm line from the Coherent Model 599 dye laser were used. The former line was used unless otherwise stated. A specially designed electrochemical Raman cell was used for the surface Raman measurements under the microscope.<sup>5</sup> A silver working electrode, which consisted of a silver rod of 5 mm diameter and 15 mm length, sealed inside an 8 mm diameter Teflon sheath, was polished with 0.5 and 0.3  $\mu\text{m}$  alumina slurries on Metron cloths. A platinum wire and a silver wire were used for a counter electrode and reference electrode,

respectively. The inner solution of the reference electrode was 0.5 M NaI aqueous solution having the same pH as that of the sample solution, and was separated from the latter solution by an agar salt bridge made of 1 M potassium chloride solution. Bulk liquids were contained in 1.5 mm glass capillary tubes for spectral measurements.

DABCO (Aldrich) and other chemicals used in the experiments were of high purity. Solutions were prepared using Milli-Q water.

## **Results and Discussion**

### **Surface Raman Spectra of DABCO-NaI Solutions with Three Different pH Values**

Raman spectra of the silver electrode surface were measured using three aqueous solutions containing 0.5 M sodium iodide and 0.1 M DABCO with pH values of 10.77, 6.23 and 0.23, adjusted with perchloric acid. Before the measurements the silver metal was roughened with several oxidation/reduction cycles. Typical Raman spectra of the 50-500  $\text{cm}^{-1}$  region are shown in Fig. 1. For the alkaline solution, the spectrum consists of a small band, maximizing at 110  $\text{cm}^{-1}$ , as shown in Figure 1-A. For the acidic solution, shown in Figure 1-C, two additional peaks at 220 and 160  $\text{cm}^{-1}$  are observed and the peak at 110  $\text{cm}^{-1}$  is strongly enhanced. When the pH of the solution was 6.23, the Raman spectrum, shown in Figure 1-B-1, was obtained; it is essentially similar to that of the alkaline solution, but the band at 220  $\text{cm}^{-1}$  increased with the irradiation time in the laser beam. Fig. 1-B-2 is the spectrum after 60 min. of irradiation with the 514.5 nm laser beam. DABCO and its protonated ions have no Raman vibrational bands in the spectral region less than 300  $\text{cm}^{-1}$ ; the bands shown in Fig. 1 are related to iodide species.

### **Photochemical Decomposition of Silver Iodide**

When silver metal was polished to a clean, bright surface and was immersed in a solution of 1 M sodium iodide, the surface immediately oxidized and a silver iodide film formed

on it. This sample, in air, gave the Raman spectra shown in Figure 2. In this experiment, the surface of the sample was irradiated for a denoted time before each measurement with 100 mW of the 514.5 nm laser line. The change of the surface Raman spectrum indicates that freshly prepared silver iodide has only one peak at  $110\text{ cm}^{-1}$  but another peak appeared at about  $230\text{ cm}^{-1}$  and increased as the irradiation time was lengthened. The peak at  $110\text{ cm}^{-1}$  is assigned to the vibration of silver iodide.<sup>6</sup> The Raman spectrum of an iodine crystal (Figure 3-D) confirms that  $\text{I}_2$  gives the line at  $230\text{ cm}^{-1}$  (the line at  $420\text{ cm}^{-1}$  in Fig. 3-D is an overtone).<sup>7</sup> The difference between 215 and  $230\text{ cm}^{-1}$  is attributed to the substrata: bulk crystal or silver metal. The redox reaction of the silver iodide to give iodine and silver by light irradiation is suggested from these facts. This reaction is familiar as the principle of photography.

A similar measurement was carried out with silver metal covered with a silver iodide film in 0.5 M NaI aqueous solution by irradiating with a 100 mW 514.5 nm laser beam. This experiment showed no dependence of the Raman spectrum upon the irradiation time; no 215 (or 230)  $\text{cm}^{-1}$  iodine line appeared even after 90 min. of irradiation. These experimental results are explained by the following scheme:



The second reaction indicates that the photoproduced-iodine reacts with the iodide ion coming from bulk solution to form triiodide ion and diffuses away into the solution, thus not being present to give a surface Raman spectrum. For the in situ surface Raman measurement, the microscope was focused on the silver surface through the window of the spectroelectrochemical cell. Thus the major information came from a thin layer near the silver surface and little information came from the bulk solution. The model expressed by Eq. (1) and (2) seems reasonable.

The Raman spectrum of a solution containing  $I_3^-$  ion prepared by dissolving 0.05 mol  $I_2$  in 1 M NaI solution was measured using the 633.1 nm laser line; this solution was strongly colored. The Raman spectrum is shown in Figure 3-B. Figure 3-C is the Raman spectrum of 1 M NaI solution. Comparison of Fig. 3-B with Fig. 3-C indicates that  $I_3^-$  ion has a line at  $120\text{ cm}^{-1}$  with a shoulder at  $160\text{ cm}^{-1}$ . The line at  $120\text{ cm}^{-1}$  has been assigned to the symmetric stretching vibration of  $I_3^-$  ion, and that at  $160\text{ cm}^{-1}$ , to the asymmetric stretching vibration.<sup>6-8</sup> Thus the line observed at  $160\text{ cm}^{-1}$  of Fig. 1-C (which is shown in Fig. 3-A, again) arises from the asymmetric stretching vibration of  $I_3^-$  ion and the very intense line observed at  $110\text{ cm}^{-1}$  is a superposition of the symmetric stretching vibration of  $I_3^-$  ion and that of silver iodide.

The  $I_3^-$  ion was detected only by the surface Raman measurement and only from acidic solution. A freshly prepared acidic solution was colorless and did not contain any  $I_3^-$  ion. These facts suggest that the  $I_3^-$  ion explaining Fig. 1-C (3-A) was not a dissolved species in the bulk of the sample solution, but was a species fixed on the silver metal surface; it was detected only when the microscope was focussed on the surface.

#### **Cooperative Deposition of Diprotonated DABCO Triiodide on the Silver Metal Surface**

DABCO is a diamine and can exist in three forms in aqueous solution.

In the solutions with pH 10.77, 6.23, and 0.23 the major species of DABCO are the unprotonated form, the monoprotonated ( $\text{DABCO-H}^+$ ), and the diprotonated ( $\text{DABCO-H}_2^{2+}$ ), respectively. In the acidic solution, the diprotonated species seems to play an important role in fixing the  $I_3^-$  ion on the silver surface as a counter cation.



On the other hand, there is no evidence of the presence of monoprotonated DABCO triiodide on the silver surface in the Raman spectrum of the near neutral solution (Fig. 1-B).



Furthermore, in alkaline solution no signals from unprotonated molecular DABCO were observed and hence it appears not to fix the triiodide ion on the silver surface. Signals from the triiodide ion and  $\text{DABCO-H}_2^{2+}$  were observed in the surface Raman spectrum only for the acidic solution.

#### **Effect of Electrode Potential on Adsorption of Species**

Cyclic voltammograms of 0.5 M NaI, 0.1 M DABCO solutions with pH 10.72, 5.40 and 0.93 are shown in Figure 4. The potential of the working electrode was measured against a silver/silver iodide electrode separated from the sample solution by the salt bridge, where the inner solution of the reference electrode was 0.5 M NaI with the same pH as the sample solution, but DABCO-free. The voltammogram of the alkaline or the pH  $\approx$  5.40 solution has an equilibrium potential near zero volt. Even a little anodic polarization causes oxidation current to flow. In the alkaline solution, a mixture of silver iodide and silver hydroxide seems to cover the electrode surface; but in the pH 5.40 solution, only silver iodide is expected. The oxidation current continuously increased for the alkaline solution (Fig. 4-A); but it decreased again after passing a maximum oxidation current at +0.05 V for the pH 5.40 solution (Fig. 4-B). This suggests that the silver iodide film passivates the surface but the silver hydroxide film does not form a protective layer. At cathodic scan, all voltammograms show a reduction current maximum and a following degradation. After the reduction of adsorbed silver ion no Faradaic current flow was observed up to the potential of hydrogen evolution.

The cyclic voltammogram of the solution with pH 0.93 differs from those of pH 10.72 and pH 5.40. The oxidation current commences at -0.08 V, compared to ca. 0 V for the pH 5.40 or the alkaline solution. This cyclic voltammogram, Fig. 4-C, is interpreted as a combination of two independent voltammograms: one contribution, shown by the hatched lines in Fig. 4-C, is obviously the same as that of Fig. 4-B. This contribution comes from the silver/silver iodide redox couple. The other contribution, giving large oxidation/reduction

peaks, is attributed to the diprotonated DABCO triiodide species. It is reasonable to suppose that the latter redox reaction occurs on the illuminated region of the silver electrode where the laser is focussed, while the former redox reaction occurs on the dark regions of the electrode.

The corresponding Raman spectra at several applied potentials can be seen in Figures 5 to 10 for the three solutions. Three bands are observed in the 50-500  $\text{cm}^{-1}$  region: 110, 160 and 220  $\text{cm}^{-1}$ . The Raman spectrum of the alkaline solution was almost the same as that of the neutral solution. The sharp peaks at 105 or 109  $\text{cm}^{-1}$  were observed at anodic potential, +100 mV. This band is ascribed to the stretching vibration of silver iodide adsorbed on silver. But this peak disappeared and only a shoulder was observable at more negative potentials. This low intensity shoulder at 113  $\text{cm}^{-1}$  may be ascribed to adsorbed iodide ion on the reduced silver metal surface. For the solution with pH 5.20, another peak at 212  $\text{cm}^{-1}$ , ascribed to iodine, was observed only at +100 mV. At negative potentials the silver cation of silver iodide is electrochemically reduced; thus the photodecomposition of silver iodide cannot occur, and no iodine is expected at such potentials. On the other hand, in the alkaline solution, the film covering the electrode seems to be mainly silver hydroxide. Thus the possibility of photodecomposition of silver iodide and the observation of an iodine band is small, even at anodic potentials; thus no detectable peak of iodine was observed in Figure 5.

In Figure 7, where the Raman spectra of the acidic solutions are shown, the band ascribed to  $\text{I}_3^-$  and that to iodine can be seen, even at -100 mV, at 160 and 220  $\text{cm}^{-1}$  respectively. This observation is very reasonable when the cyclic voltammogram shown in Fig. 4-C is interpreted. It suggests that the diprotonated DABCO triiodide giving these peaks is stable up to about -100 mV. The oxidation wave at -50 mV and the reduction wave at -150 mV relate to the following reactions:



The net reaction can be expressed as follows



And the equilibrium potential of this total reaction seems to exist at a potential near -100 mV.

In Figure 8, 9, and 10, surface Raman spectra of the 500 to 950  $\text{cm}^{-1}$  region are shown for these solutions. Intensities were very weak and thus the spectra show a low signal-to-noise ratio. A 800  $\text{cm}^{-1}$  peak observed for almost all spectra has been ascribed to the cage-breathing vibration of a DABCO species.<sup>4</sup> A splitting of this peak was observed at +100 and -100 mV for acidic (pH 0.85) solution, as shown in Figure 10-A,B; at more negative potentials, including -150 and -300 mV, the splitting did not appear, as shown in Fig. 10-C and D. The splitting of the peak suggests that the diprotonated DABCO exists in two different environments. They could be the free species and a surface-fixed species of diprotonated DABCO triiodide.

A photograph of the crystal formed at the focal point of the laser beam on the electrode is shown in Figure 11; this was taken after keeping the silver electrode at +100 mV for three hours under 514.5 nm 300 mW laser irradiation in the solution with pH 0.93. Every needle-like crystal is growing from the focal point. These crystals were stable and unchanged even at -100 mV. When the electrode potential was made more cathodic, e.g. up to -150 mV, these crystals disappeared immediately and completely. The -150 mV was the potential at which the large cathodic current of Fig. 4-C started to flow. Crystals were not found when diprotonated DABCO was absent. Unfortunately, the size of the crystal was too small for elemental analysis.

In summary, the phenomena occurring on the silver electrode, when in contact with the acidic solution, are illustrated in Fig. 12. The following steps would proceed only at a potential

more positive than -150 mV and only in acidic solution. As step 1, electrochemically formed silver iodide is photodecomposed to atomic silver and iodine. The atomic iodine can form a triiodide ion with another iodide ion coming from bulk solution (step 2); it is fixed on the electrode surface to make an ion-pair with a diprotonated DABCO cation (step 3). Another silver iodide is photodecomposed and the steps 1-3 are repeated. This results in the growth of the diprotonated DABCO triiodide crystal. This crystal has a stoichiometry and structure similar to the polyiodide of DIPSPH<sub>4</sub> (tetraphenyldithiapyranylidene).<sup>10,11</sup> Crystals of organic polyiodides are reported to have high conductivity.<sup>7,9-12</sup>

#### **Acknowledgement**

This work was supported by grants from the Natural Sciences and Engineering Research Council of Canada and the Office of Naval Research.

## **References**

1. Irish, D.E.; Guzonas, D.A.; Atkinson, G.F. *Surf. Sci.* **1985**, 158, 314.
2. Guzonas, D.A.; Irish, D.E.; Atkinson, G.F. *Langmuir* **1990**, 6, 1102.
3. Guzonas, D.A.; Irish, D.E.; Atkinson, G.F. *Langmuir* **1989**, 5, 787.
4. Guzonas, D.A.; Irish, D.E. *Can. J. Chem.* **1988**, 66, 1249.
5. Ozeki, T.; Irish, D.E. *J. Electroanal. Chem.* **1990**, 280, 451.
6. Weiss, G.S.; Parkes, A.S.; Nixon, E.R.; Hughes, R.E. *J. Chem. Phys.* **1964**, 41, 3759.
7. Marks, T.J.; Webster, D.F. *J. Chem. Soc. Chem. Commun.* **1976**, 444.
8. Maki, A.G.; Forneris, R. *Spectrochimica Acta* **1967**, 23A, 867.
9. Abkowitz, M.A.; Epstein, A.J.; Griffiths, C.H.; Miller, J.S.; Slade, M.L. *J. Am. Chem. Soc.* **1977**, 99, 5304.
10. Bandrauk, A.D.; Ishii, K.; Truong, K.D.; Aubin, M.; Hanson, A.W. *J. Phys. Chem.* **1985**, 89, 1478.
11. Bandrauk, A.D.; Truong, K.D.; Carlone, C.; Hanson, A.W. *J. Phys. Chem.* **1987**, 91, 2063.
12. Petersen, J.L.; Schramm, C.S.; Stojakovic, D.R.; Hoffman, B.M.; Marks, T.J. *J. Am. Chem. Soc.* **1977**, 99, 2286.

**Figure Captions**

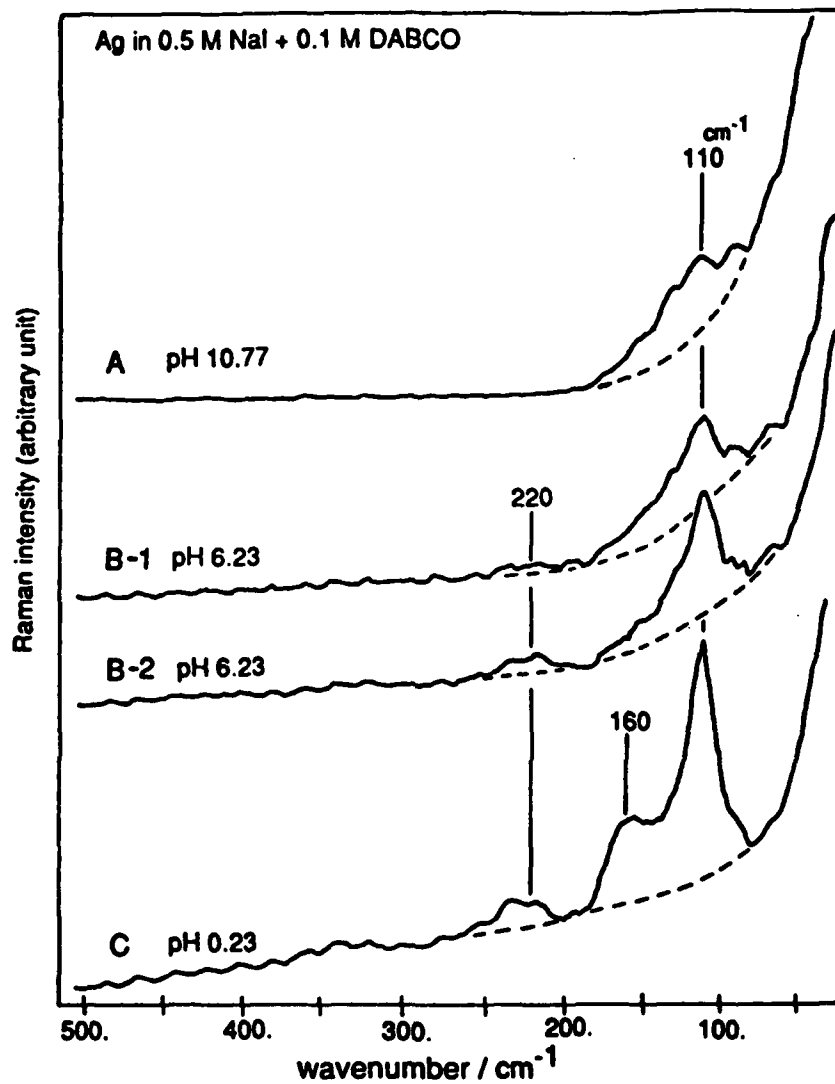
- Figure 1: Surface Raman spectra of silver metal in 0.5 M NaI and 0.1 M DABCO solutions with A: pH 10.77, B: pH 6.23 and C: pH 0.23. B-2 is the spectrum after irradiation with laser light of 514.5 nm and 100 mW for 60 min.
- Figure 2: Surface Raman spectra of silver metal covered by a silver iodide film, in contact with air, after 514.5 nm laser beam irradiation for A: 0, B: 60, C: 90, and D: 120 min.
- Figure 3: Comparison of several Raman spectra; A: surface Raman spectrum of silver metal in 0.5 M NaI and 0.1 M DABCO solution with pH 0.23; B: bulk Raman spectrum of a solution of 1 M NaI and 0.05 M I<sub>2</sub>; C: bulk Raman spectrum of a solution of 1 M NaI; and D: surface Raman spectrum of pure iodine crystal.
- Figure 4: Cyclic voltammograms of the solutions of 0.5 M NaI and 0.1 M DABCO with A: pH 10.72, B: pH 5.40, and C: pH 0.93, respectively. Scan rate is 10 mV/s.
- Figure 5: Dependence of the surface Raman spectrum of the silver electrode in the 50-500 cm<sup>-1</sup> region on the electrode potential for 0.5 M NaI and 0.1 M DABCO solution with pH 10.14.
- Figure 6: Dependence of the surface Raman spectrum of the silver electrode in the 50-500 cm<sup>-1</sup> region on the electrode potential for 0.5 M NaI and 0.1 M DABCO solution with pH 5.20.
- Figure 7: Dependence of the surface Raman spectrum of the silver electrode in the 50-500 cm<sup>-1</sup> region on the electrode potential for 0.5 M NaI and 0.1 M DABCO solution with pH 0.85.
- Figure 8: Dependence of the surface Raman spectrum of the silver electrode in the 500-950 cm<sup>-1</sup> region on the electrode potential for 0.5 M NaI and 0.1 M DABCO solution with pH 10.14.

Figure 9: Dependence of the surface Raman spectrum of the silver electrode in the 500-950  $\text{cm}^{-1}$  region on the electrode potential for the 0.5 M NaI and 0.1 M DABCO solution with pH 5.20.

Figure 10: Dependence of the surface Raman spectrum of the silver electrode in the 500-950  $\text{cm}^{-1}$  region on the electrode potential for the 0.5 M NaI and 0.1 M DABCO solution with pH 0.85.

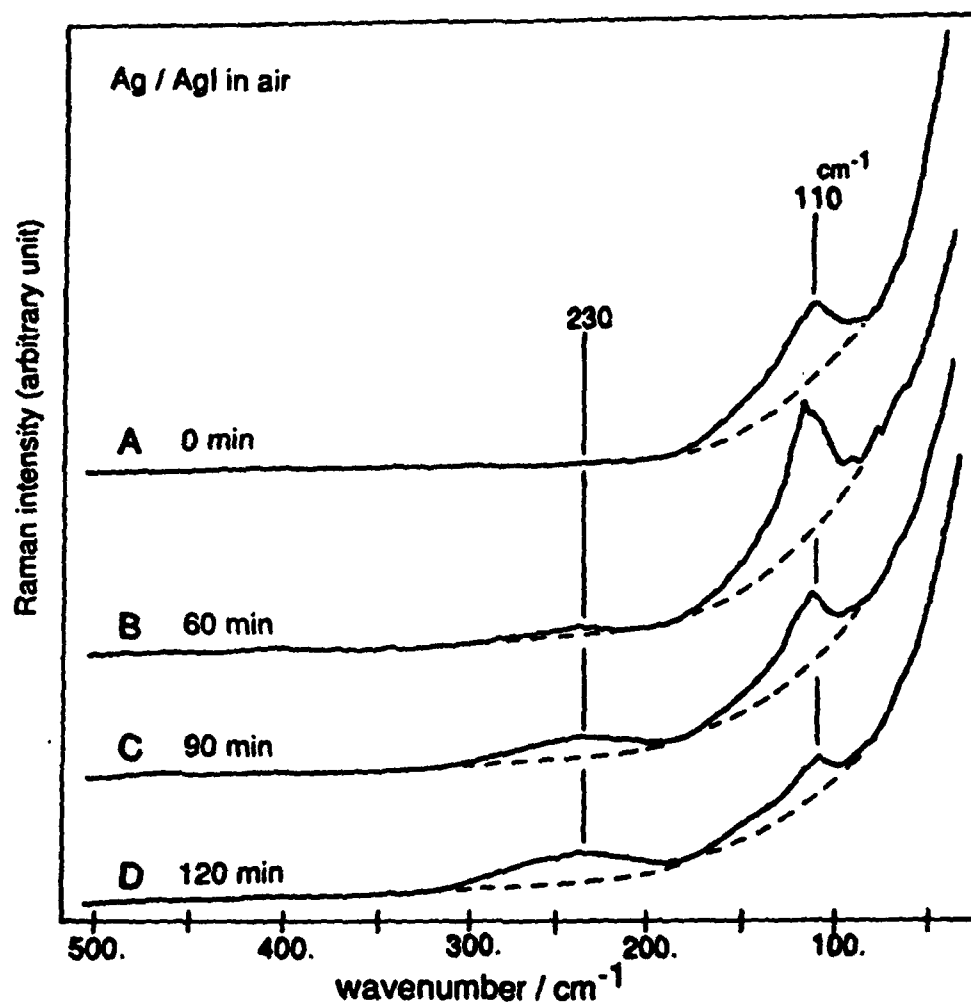
Figure 11: A typical diprotonated DABCO triiodide crystal formed upon the silver electrode after being kept at +100 mV vs. Ag/AgI for 3 h with 514.5 nm 300 mW laser irradiation.

Figure 12: Schematic illustration of the mechanism for the formation of the diprotonated DABCO triiodide crystal on the silver electrode.



**Figure 1:** Surface Raman spectra of silver metal in 0.5 M NaI and 0.1 M DABCO solutions with A: pH 10.77, B: pH 6.23 and C: pH 0.23. B-2 is the spectrum after irradiation with laser light of 514.5 nm and 100 mW for 60 min.





**Figure 2:** Surface Raman spectra of silver metal covered by a silver iodide film, in contact with air, after 514.5 nm laser beam irradiation for A: 0, B: 60, C: 90, and D: 120 min.

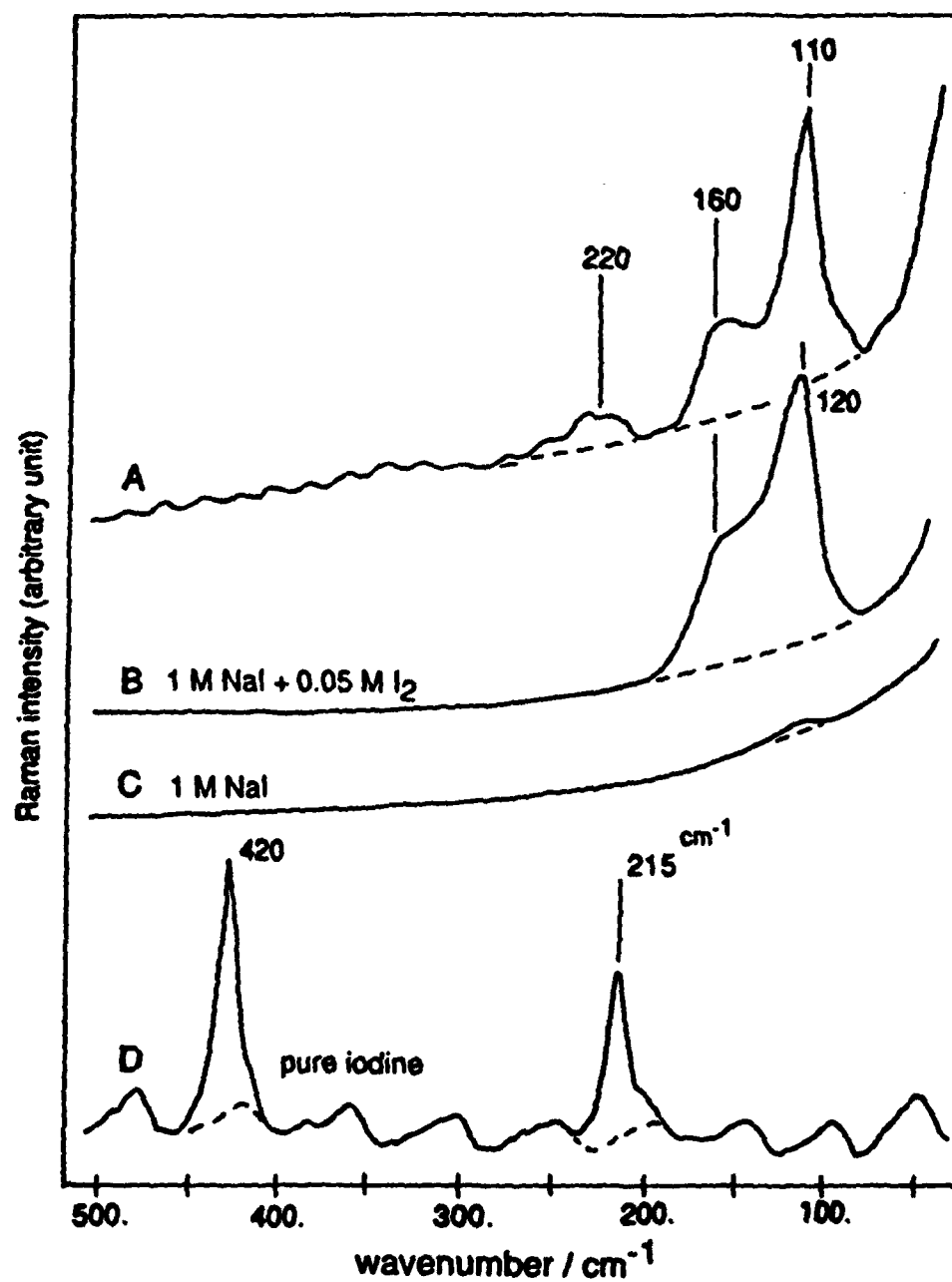


**Figure 3:** Comparison of several Raman spectra; A: surface Raman spectrum of silver metal in 0.5 M NaI and 0.1 M DABCO solution with pH 0.23; B: bulk Raman spectrum of a solution of 1 M NaI and 0.05 M  $\text{I}_2$ ; C: bulk Raman spectrum of a solution of 1 M NaI; and D: surface Raman spectrum of pure iodine crystal.

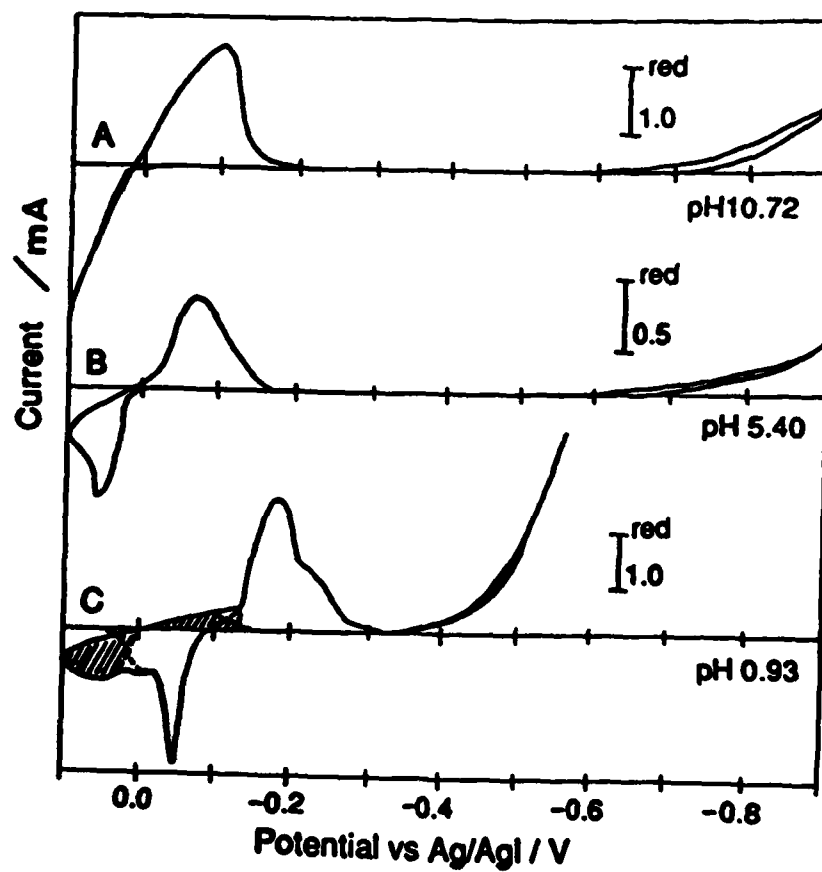


**Figure 4:** Cyclic voltammograms of the solutions of 0.5 M NaI and 0.1 M DABCO with A: pH 10.72, B: pH 5.40, and C: pH 0.93, respectively. Scan rate is 10 mV/s.

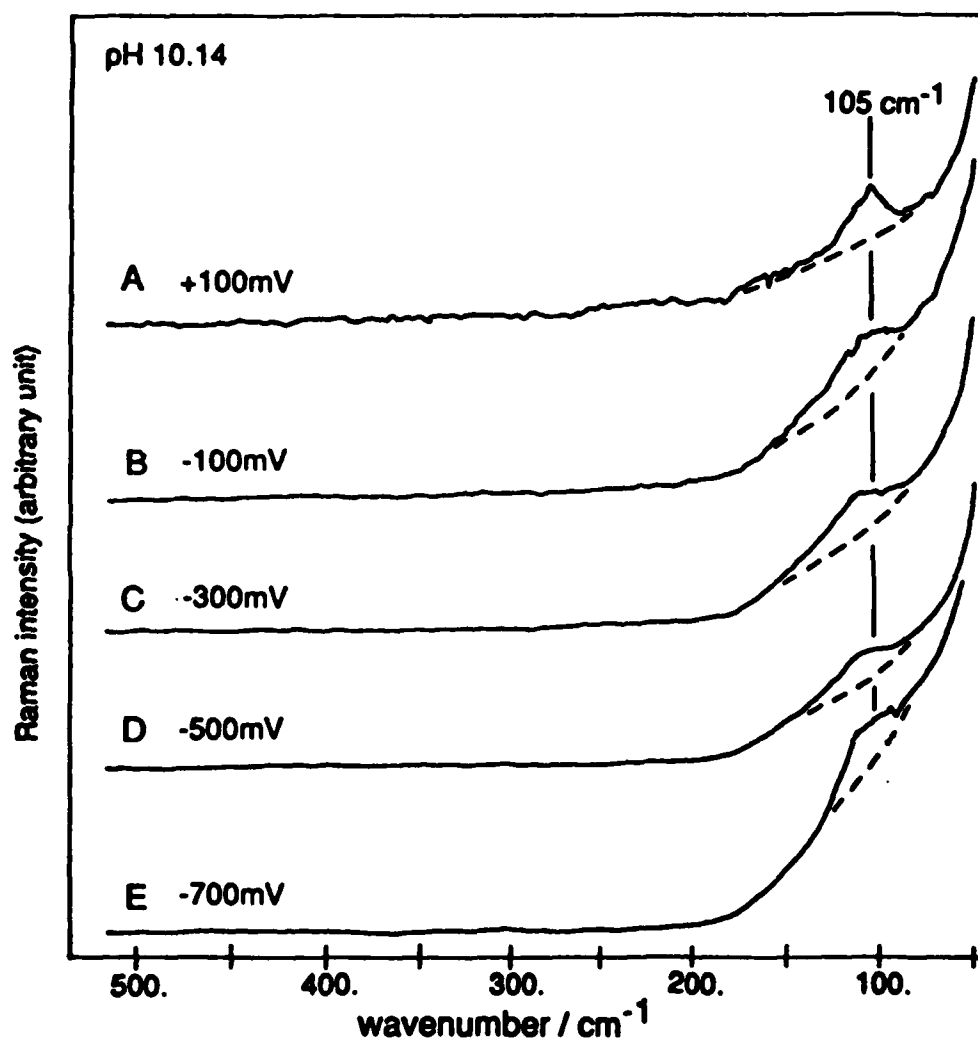


**Figure 5:** Dependence of the surface Raman spectrum of the silver electrode in the 50-500  $\text{cm}^{-1}$  region on the electrode potential for 0.5 M NaI and 0.1 M DABCO solution with pH 10.14.

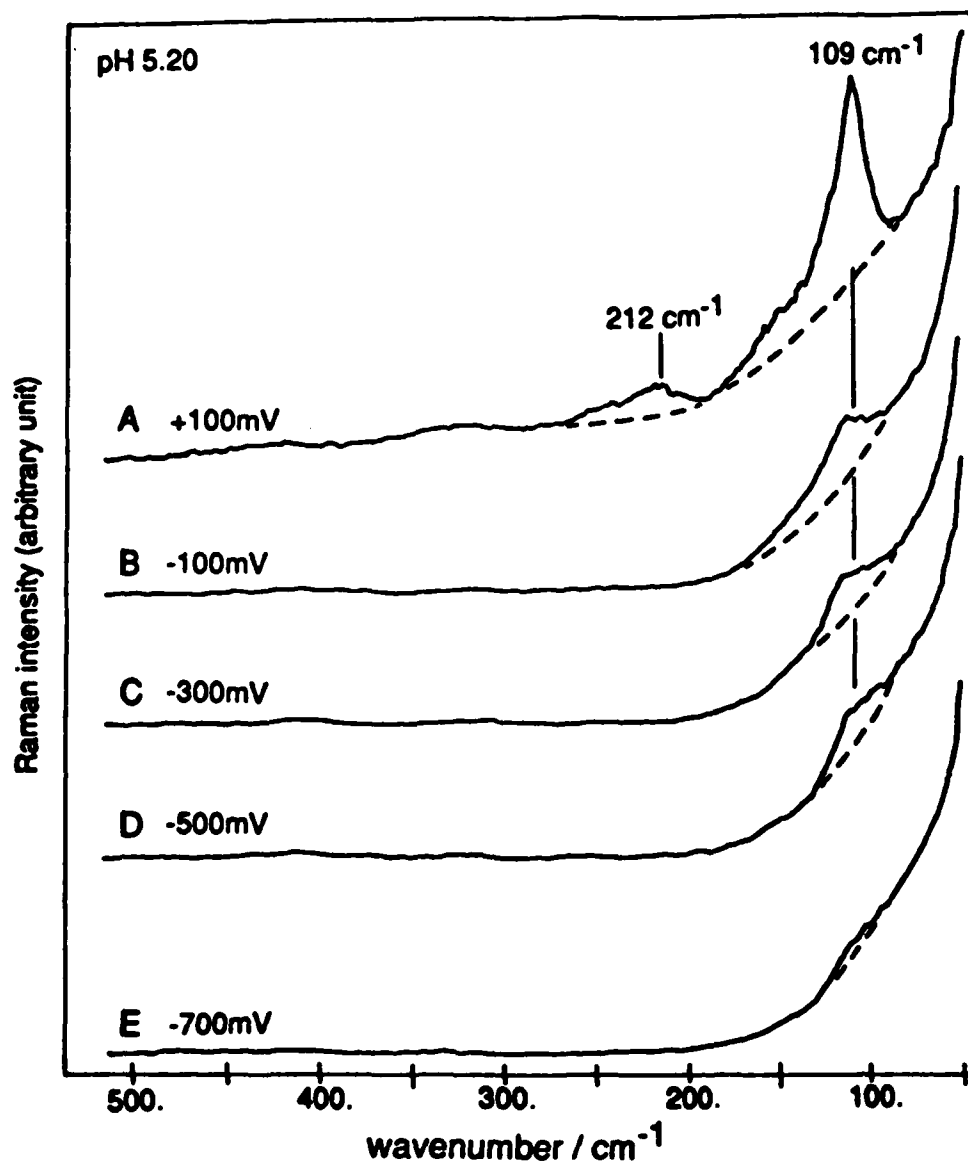


**Figure 6:** Dependence of the surface Raman spectrum of the silver electrode in the 50-500  $\text{cm}^{-1}$  region on the electrode potential for 0.5 M NaI and 0.1 M DABCO solution with pH 5.20.

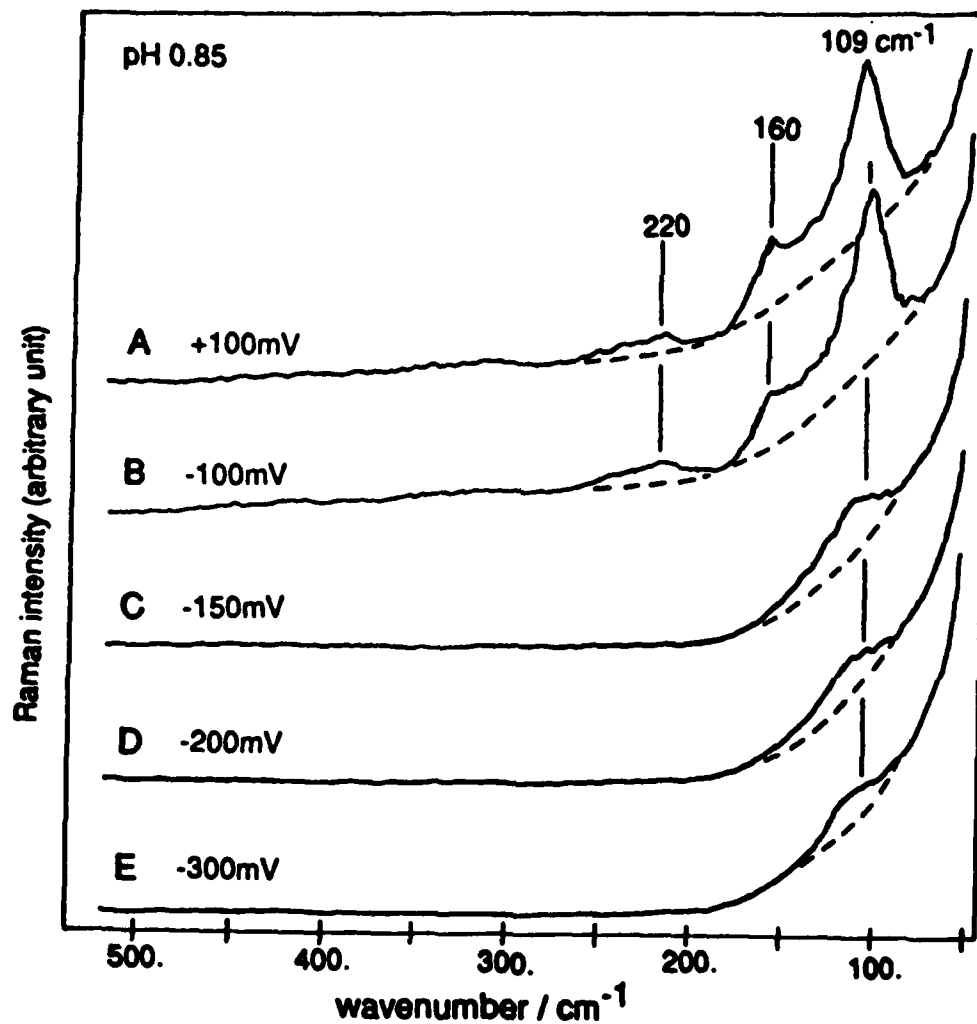


**Figure 7:** Dependence of the surface Raman spectrum of the silver electrode in the 50-500 cm<sup>-1</sup> region on the electrode potential for 0.5 M NaI and 0.1 M DABCO solution with pH 0.85.

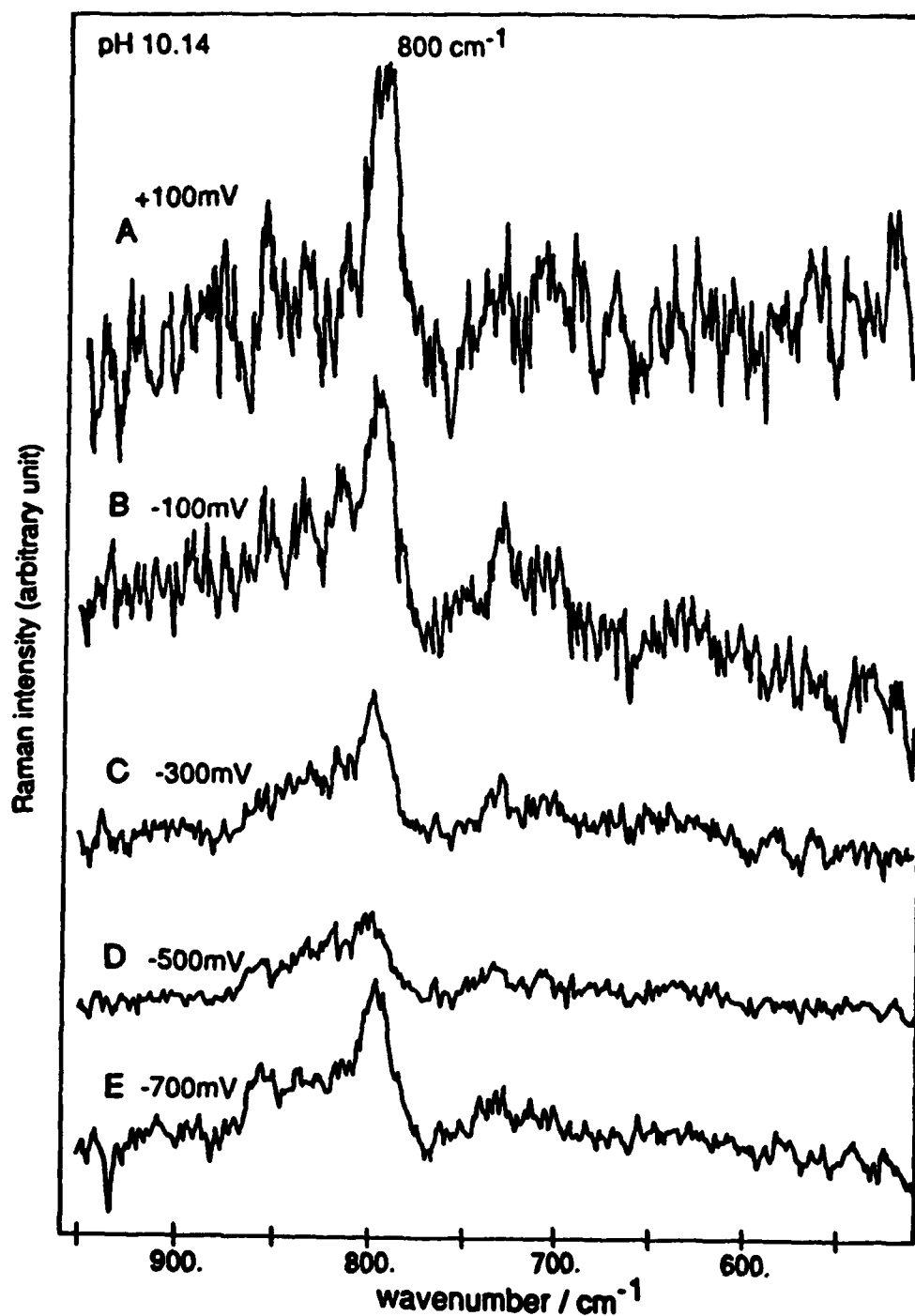


**Figure 8:** Dependence of the surface Raman spectrum of the silver electrode in the 500-950  $\text{cm}^{-1}$  region on the electrode potential for 0.5 M NaI and 0.1 M DABCO solution with pH 10.14.

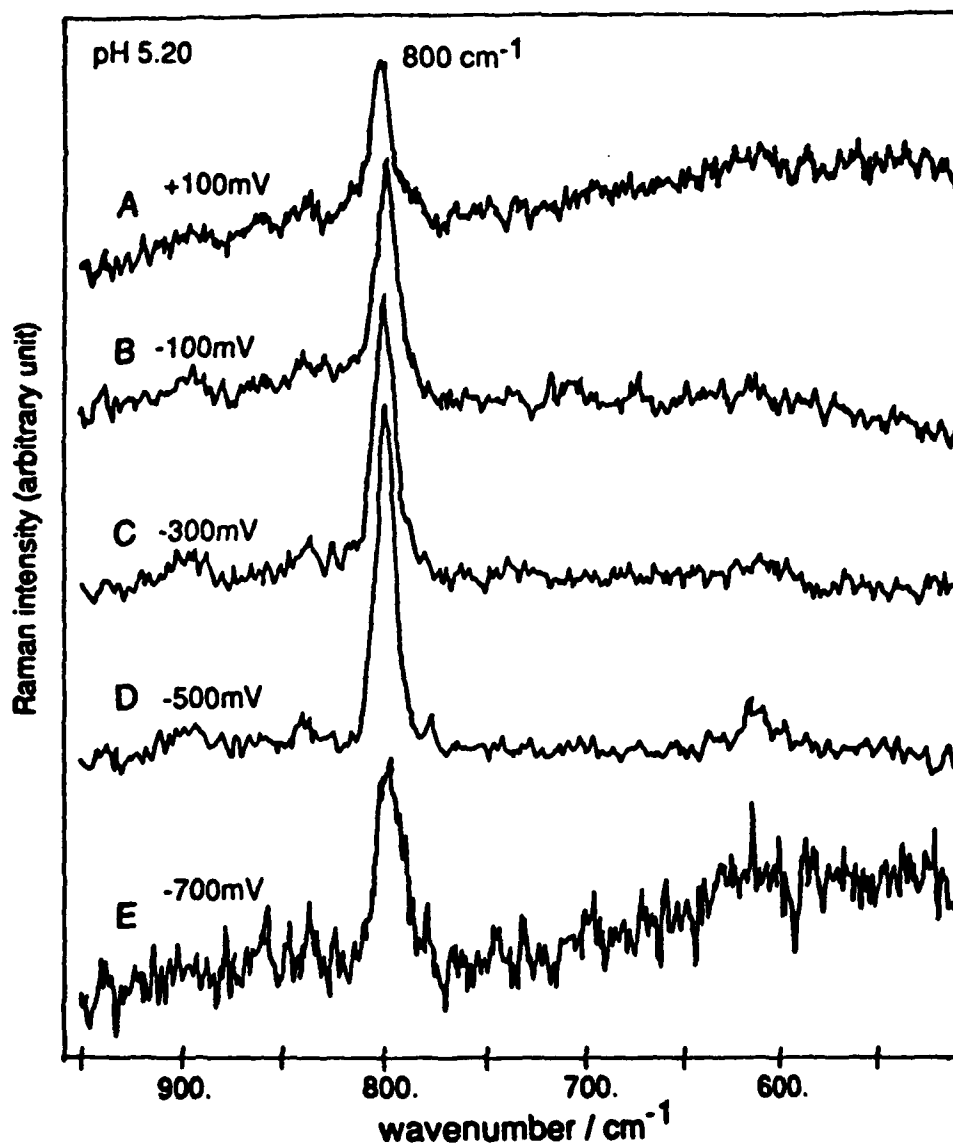


**Figure 9:** Dependence of the surface Raman spectrum of the silver electrode in the 500-950  $\text{cm}^{-1}$  region on the electrode potential for the 0.5 M NaI and 0.1 M DABCO solution with pH 5.20.



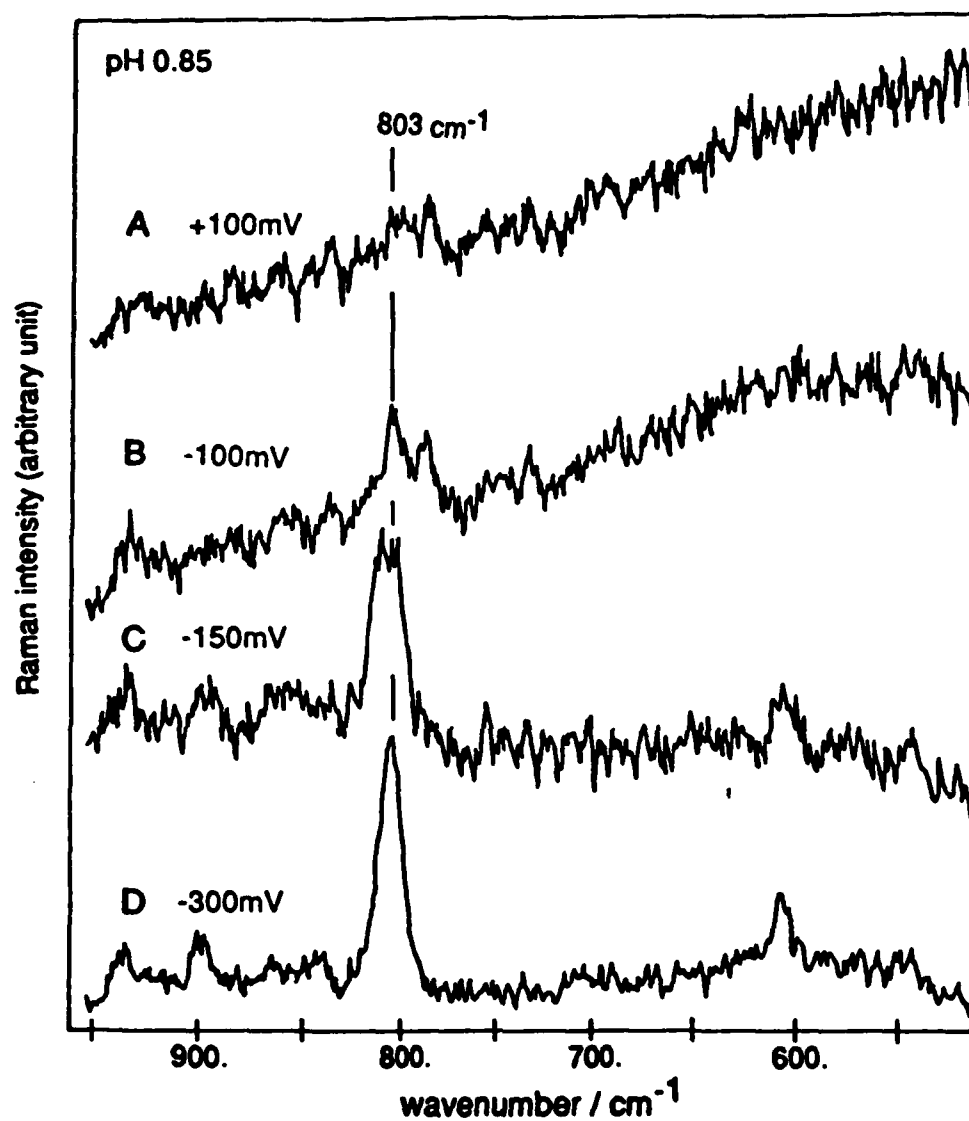


**Figure 10:** Dependence of the surface Raman spectrum of the silver electrode in the 500-950  $\text{cm}^{-1}$  region on the electrode potential for the 0.5 M NaI and 0.1 M DABCO solution with pH 0.85.

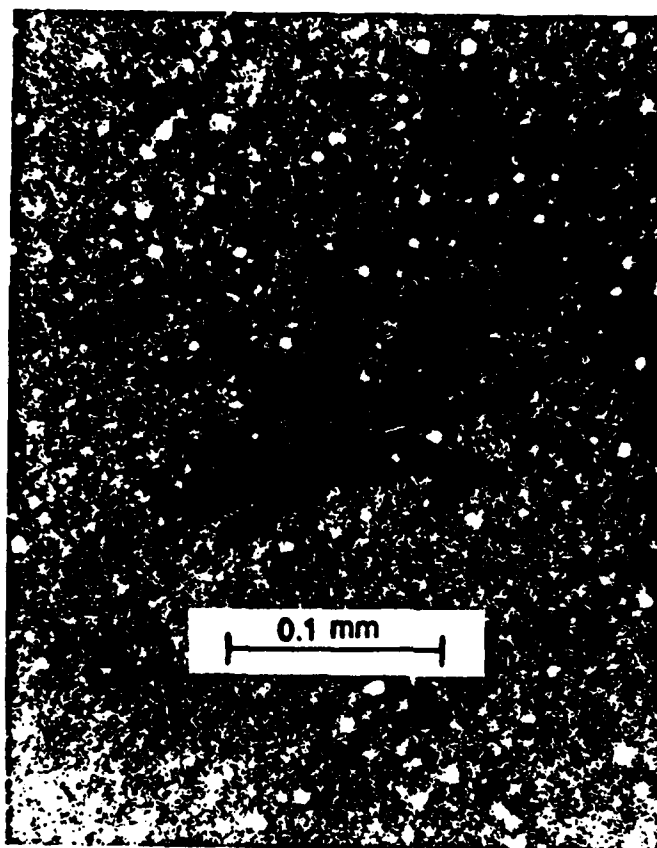


**Figure 11:** A typical diprotonated DABCO triiodide crystal formed upon the silver electrode after being kept at +100 mV vs. Ag/AgI for 3 h with 514.5 nm 300 mW laser irradiation.

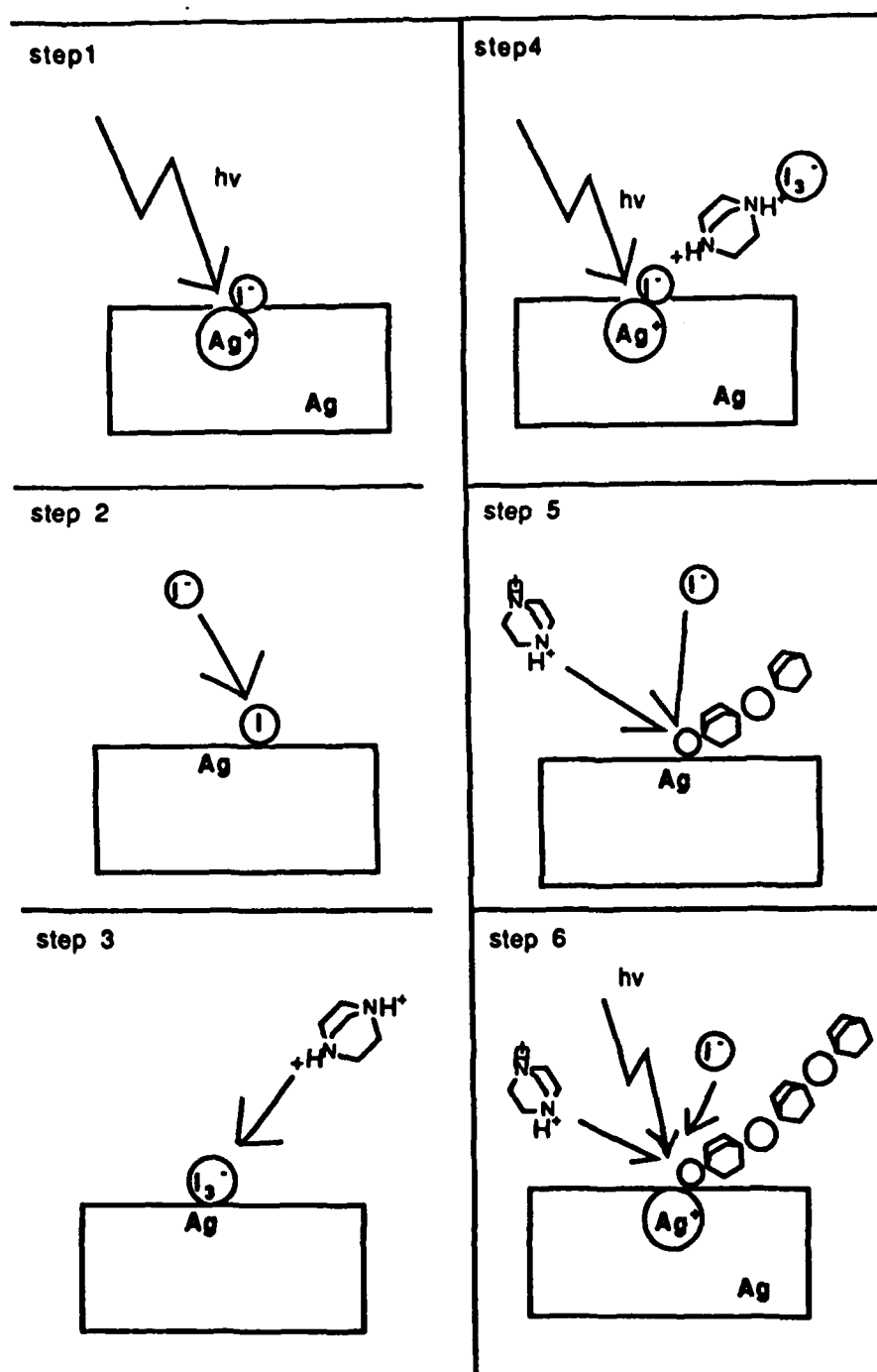


**Figure 12:** Schematic illustration of the mechanism for the formation of the diprotonated DABCO triiodide crystal on the silver electrode.

TECHNICAL REPORT DISTRIBUTION LIST - GENERAL

Office of Naval Research (2)  
Chemistry Division, Code 1113  
800 North Quincy Street  
Arlington, Virginia 22217-5000

Commanding Officer (1)  
Naval Weapons Support Center  
Dr. Bernard E. Douda  
Crane, Indiana 47522-5050

Dr. Richard W. Drisko (1)  
Naval Civil Engineering  
Laboratory  
Code L52  
Port Hueneme, CA 93043

David Taylor Research Center (1)  
Dr. Eugene C. Fischer  
Annapolis, MD 21402-5067

Dr. James S. Murday (1)  
Chemistry Division, Code 6100  
Naval Research Laboratory  
Washington, D.C. 20375-5000

Defence Technical Information (2)  
Center  
Building 5  
Cameron Station  
Alexandria, VA  
U.S.A. 22314

Dr. Robert Green, Director (1)  
Chemistry Division, Code 385  
Naval Weapons Center  
China Lake, CA 93555-6001

Chief of Naval Research (1)  
Special Assistant for Marine  
Corps Matters  
Code 00MC  
800 North Quincy Street  
Arlington, VA 22217-5000

Dr. Bernadette Eichinger (1)  
Naval Ship Systems Engineering  
Station  
Code 053  
Philadelphia Naval Base  
Philadelphia, PA 19112

Dr. Sachio Yamamoto (1)  
Naval Ocean Systems Center  
Code 52  
San Diego, CA 92152-5000

Dr. Harold H. Singerman (1)  
David Taylor Research Center  
Code 283  
Annapolis, MD 21402-5067

ENCLOSURE(2)